Biochimica et Biophysica Acta 1827 (2013) 411–419

Contents lists available at SciVerse ScienceDirect

Biochimica et Biophysica Acta

journal homepage: www.elsevier.com/locate/bbabio

High-light vs. low-light: Effect of light acclimation on photosystem II composition and organization in *Arabidopsis thaliana*

Roman Kouřil [a,b,*], Emilie Wientjes [c], Jelle B. Bultema [a,1], Roberta Croce [c], Egbert J. Boekema [a]

[a] Department of Biophysical Chemistry, Groningen Biomolecular Sciences and Biotechnology Institute, University of Groningen, Nijenborgh 7, 9747 AG Groningen, The Netherlands
[b] Centre of the Region Haná for Biotechnological and Agricultural Research, Department of Biophysics, Faculty of Science, Palacký University, Šlechtitelů 11, 783 71 Olomouc, Czech Republic
[c] Department of Physics and Astronomy, Faculty of Sciences, VU University Amsterdam, De Boelelaan 1081, 1081 HV Amsterdam, The Netherlands

ARTICLE INFO

Article history:
Received 6 November 2012
Received in revised form 11 December 2012
Accepted 14 December 2012
Available online 27 December 2012

Keywords:
Photosystem II supercomplex
Thylakoid membrane
Electron microscopy
Light acclimation

ABSTRACT

The structural response of photosystem II (PSII) and its light-harvesting proteins (LHCII) in *Arabidopis thaliana* after long-term acclimation to either high or low light intensity was characterized. Biochemical and structural analysis of isolated thylakoid membranes by electron microscopy indicates a distinctly different response at the level of PSII and LHCII upon plant acclimation. In high light acclimated plants, the $C_2S_2M_2$ supercomplex, which is the dominating form of PSII in *Arabidopsis*, is a major target of structural re-arrangement due to the down-regulation of Lhcb3 and Lhcb6 antenna proteins. The PSII ability to form semi-crystalline arrays in the grana membrane is strongly reduced compared to plants grown under optimal light conditions. This is due to the structural heterogeneity of PSII supercomplexes rather than to the action of PsbS protein as its level was unexpectedly reduced in high light acclimated plants. In low light acclimated plants, the architecture of the $C_2S_2M_2$ supercomplex and its ability to form semi-crystalline arrays remained unaffected but the density of PSII in grana membranes is reduced due to the synthesis of additional LHCII proteins. However, the $C_2S_2M_2$ supercomplexes in semi-crystalline arrays are more densely packed, which can be important for efficient energy transfer between PSII under light limiting conditions.

1. Introduction

Photosynthesis is carried out in the thylakoid membrane, which accommodates the photosynthetic apparatus. Photosystem II (PSII) and its accessory light harvesting complex II (LHCII) reside mainly in the stacks of thylakoids, called grana, which are interconnected by stromal thylakoids, where photosystem I (PSI) and ATP-synthase are mainly confined. They form, together with the cytochrome b_6f complex, the core of the photosynthetic apparatus [1,2].

PSII of higher plants is a multiple protein supercomplex. The core complex consists of D1 and D2 and the inner antenna proteins CP43 and CP47. A dimer of the core complex interacts with a variable number of additional light harvesting complexes (Lhcb1–6). Lhcb1–3 form several types of heterotrimers. They interact specifically with the PSII core via monomeric antenna proteins Lhcb4 (also called CP29), Lhcb5 (CP26) and Lhcb6 (CP24) to form PSII-LHCII supercomplexes (see [3] for a recent review). The largest PSII–LHCII supercomplex in *Arabidopsis*, the so-called $C_2S_2M_2$ supercomplex, consists of the PSII core dimer (C_2), two strongly bound LHCII trimers (S_2) at the side of CP26 and two moderately bound LHCII trimers (M_2), which interact with the core via CP29 and CP24 [4,5]. A 2D projection map of the $C_2S_2M_2$ supercomplex was obtained by single particle electron microscopy (EM) at 12 Å resolution [6], which allowed the reconstruction of a 3D pseudo atomic model of the PSII-LHCII and the visualization of possible energy transfer pathways in the supercomplex [7]. Biochemical evidence suggests that in the thylakoid membrane up to eight LHCII trimers can be present per PSII core dimer [8–10]. This indicates the presence of a pool of "extra" LHCII, which has unknown location with respect to PSII.

It is obvious that more detailed studies of the molecular architecture of the PSII-LHCII supercomplex are important for a deeper understanding of its role in the primary reactions of photosynthesis. There is gathering evidence that the higher organization of PSII and LHCII in the thylakoid membrane is of equal relevance for the regulation and optimization of photosynthetic process. Pioneering freeze-fracture and freeze-etch EM studies revealed first glimpses about a random or well-ordered organization of PSII complexes in the thylakoid membrane [3,11–13]. More recently, both mathematical simulations and data from atomic force microscopy confirm that the PSII distribution in the grana membranes is not completely random [14–16]. Details of the packing and the molecular composition of PSII in these arrays are known from EM analysis of negatively stained grana membranes, which revealed that the arrays consist of C_2S_2, C_2S_2M or $C_2S_2M_2$ supercomplexes [17,18]. Although factors like cold acclimation [16,19], low light acclimation [20], lack of PsbS and

* Corresponding author at: Centre of the Region Haná for Biotechnological and Agricultural Research, Department of Biophysics, Faculty of Science, Palacký University, Šlechtitelů 11, 783 71 Olomouc, Czech Republic. Tel.: +420 58 5634179; fax: +420 58 5225737.
E-mail address: roman.kouril@upol.cz (R. Kouřil).
[1] Present address: Department of Microbiology, Groningen Biomolecular Sciences and Biotechnology Institute, University of Groningen, Nijenborgh 7, 9747 AG Groningen, The Netherlands.

0005-2728/$ – see front matter © 2013 Elsevier B.V. All rights reserved.
http://dx.doi.org/10.1016/j.bbabio.2012.12.003

absence of specific Lhcb antenna proteins [21–23] were found to increase the population of semi-crystalline arrays, their physiological significance is not understood. Recently, cryo electron tomography extended our knowledge about the higher organization of PSII complexes into the third dimension, which provides, among others, unique information about the interaction between PSII complexes in adjacent layers of grana membranes [24,25]. These tomography data indicate that the formation of semi-crystalline arrays *in situ* depends on the interaction of the stroma exposed membrane surface of two adjacent layers, which both contain ordered arrays of PSII complexes [24].

In nature, plants are continuously exposed to varying environmental conditions on a daily or seasonal time scale. Light is for photosynthetic organisms which is one of the most important factors to cope with. As short-term response to varying light intensity and spectral quality, plants had to evolve different mechanisms (i) to protect themselves from photooxidative damage under high light (Non-Photochemical Quenching (NPQ), reviewed by e.g. [26]) and (ii) to optimize photosynthetic function under low light (state transitions, reviewed by e.g. [27]). There are experimental indications that these mechanisms involve structural changes at the level of PSII, LHCII and their higher organization in the thylakoid membrane [28].

Long-term acclimation to different light intensities is accompanied by a regulation of the amount of LHC proteins and PSII/PSI ratio [29]. Under high light, the amount of LHC is reduced, whereas the PSII content increases compared to PSI. The opposite effect is observed under low light, where the lower PSII/PSI ratio reflects a lower amount of PSII complexes, which associate with a larger amount of LHCII proteins [30–32]. Current structural data about the higher organization of PSII in grana membranes are limited to low light conditions, when down-regulation of the PSII content led to a formation of specifically ordered rows of PSII in the grana membrane [20].

The aim of this work is to extend our knowledge about structural aspects of long-term acclimation of plants to either high or low light intensity at the level of PSII supercomplexes and their higher organization in the thylakoid membrane of *Arabidopsis thaliana*. Biochemical analysis of plants acclimated to different light conditions indicates a specific alteration of the composition of PSII supercomplexes and the amount of LHCII proteins. Thorough analysis of electron micrographs revealed a specific response of acclimated plants at the level of both well-ordered and randomly distributed PSII supercomplexes in the thylakoid membrane. We addressed the question whether a long-term acclimation of plants to different light intensities favors the formation of semi-crystalline arrays of PSII supercomplexes in the grana membrane and whether PSII associations in such arrays are characteristic to specific light conditions. Furthermore, analysis of randomly distributed PSII supercomplexes in the grana membrane gave us information about the strategy used by the plant to acclimate to different light intensities.

2. Materials and methods

2.1. Plant material

A. thaliana (Col) plants were grown in a growth chamber (Plant Climatics Percival Growth Chamber, Model AR-36L, Germany) at 100 μE/m^2/s, 70% humidity, 22 °C, and 8 h of daylight and 16 h of dark period. After four weeks, control plants were grown for additional 2.5 weeks at 100 μE/m^2/s (NL) and plants acclimated to low light (LL) and high light (HL) were grown under 20 μE/m^2/s and 800–1100 μE/m^2/s, respectively, for additional four weeks.

2.2. Isolation of thylakoid membranes

A. thaliana leaves were harvested at the end of a dark period. Thylakoid membranes were prepared according to [33], with modifications described in [6]. The membranes were resuspended in 20 mM HEPES, pH = 7.5, 0.4 M sorbitol, 15 mM NaCl, 5 mM $MgCl_2$, quickly frozen in liquid N_2 and stored at 193 K until use.

2.3. Polyacrylamide gel electrophoresis and immunoblot analysis

SDS-PAGE was performed with the Tris–Tricine system [34] at a 14.5% acrylamide concentration. To estimate the level of Lhcb1,2 per CP29 the gels were digitized with a Fujifilm LAS 300 scanner after Coomassie Brilliant Blue staining, and the optical density integrated on the area of the CP29 and Lhcb1,2 band was quantified using the GEL-PRO Analyzer (Media Cybernetics). The number of Lhcb1,2 copies per CP29 was quantified as described by [35], as one CP29 is present per PSII core [18], this gives the Lhcb1,2/PSII core ratio. One Lhcb3 is present per M trimer [6,36,37] and thus per PSII core in NL and LL plants, while based on immunoblot analysis the Lhcb3 level is reduced to 0.5 per PSII in HL plants. These values were used to calculate the amount of LHCII trimers (Lhcb1,2 + Lhcb3)/3 per PSII core. Double amounts are present per PSII core dimer. Immunoblot analysis was performed as in [38] with antibodies from Agrisera (Sweden).

2.4. Electron microscopy of grana membranes

Prior to the solubilization step, thylakoids were thawed on ice and resuspended in an excess of buffer A (20 mM HEPES, pH = 7.5 and 5 mM $MgCl_2$) and spun down using an Eppendorf table centrifuge (5 min, max. speed, 4 °C) to remove the sorbitol. After this washing step, thylakoid membranes were solubilized using digitonin (0.5 mg of chls/ml, 0.5% digitonin in buffer A) for 20 min at 4 °C while slowly stirred, followed by centrifugation in an Eppendorf table centrifuge (5 min, max. speed, 4 °C). The pellet, with the non-solubilized grana thylakoid membranes, was washed once more with buffer A, spun down again for 5 min and then used for EM analysis.

Specimens were prepared by negative staining with 2% uranyl acetate on glow-discharged carbon-coated copper grids. Electron microscopy was performed on a Philips CM120 electron microscope equipped with a LaB_6 tip and operated at 120 kV. Images were recorded with a Gatan 4000 SP 4 K slow-scan CCD camera at 80,000 magnification with a pixel size of 0.375 nm at the specimen level after binning the images to 2048 × 2048 pixels. GRACE software was used for semi-automated data acquisition [39]. Electron micrographs were band-pass filtered prior analysis to improve an image contrast. Sub-areas of semi-crystalline arrays of PSII supercomplexes were analyzed using a single particle approach with the Groningen Image Processing (GRIP) software including reference alignments and averaging of aligned projections. Sub-areas (256 × 256 pixels) of PSII arrays were selected from individual electron micrographs and analyzed separately. To determine the minimal distance between PSII complexes and the density of PSII complexes in the membrane area, mid-mass positions of the PSII core complexes were marked manually using GRIP. To determine the minimal distance, coordinates of about 5000 PSII complexes were selected for each examined sample and analyzed with Microsoft Excel.

3. Results

3.1. Long-term acclimation to different light intensities induces changes in the composition of the PSII light harvesting antenna and modifies the level of PsbS

Biochemical analysis of plants acclimated to different light intensities revealed a diverse regulation of both the composition and size of the antenna system of PSII and also the level of the PsbS protein. The modification in the content of CP24, CP29 and Lhcb3 (a component of the M trimer of LHCII) was monitored by immunoblotting and normalized to the amount of Chl content and CP43 (a PSII core protein). Fig. 1 shows that in HL plants the level of CP43/Chl was significantly higher than in both NL and LL plants, due to a reduced level of LHCII proteins

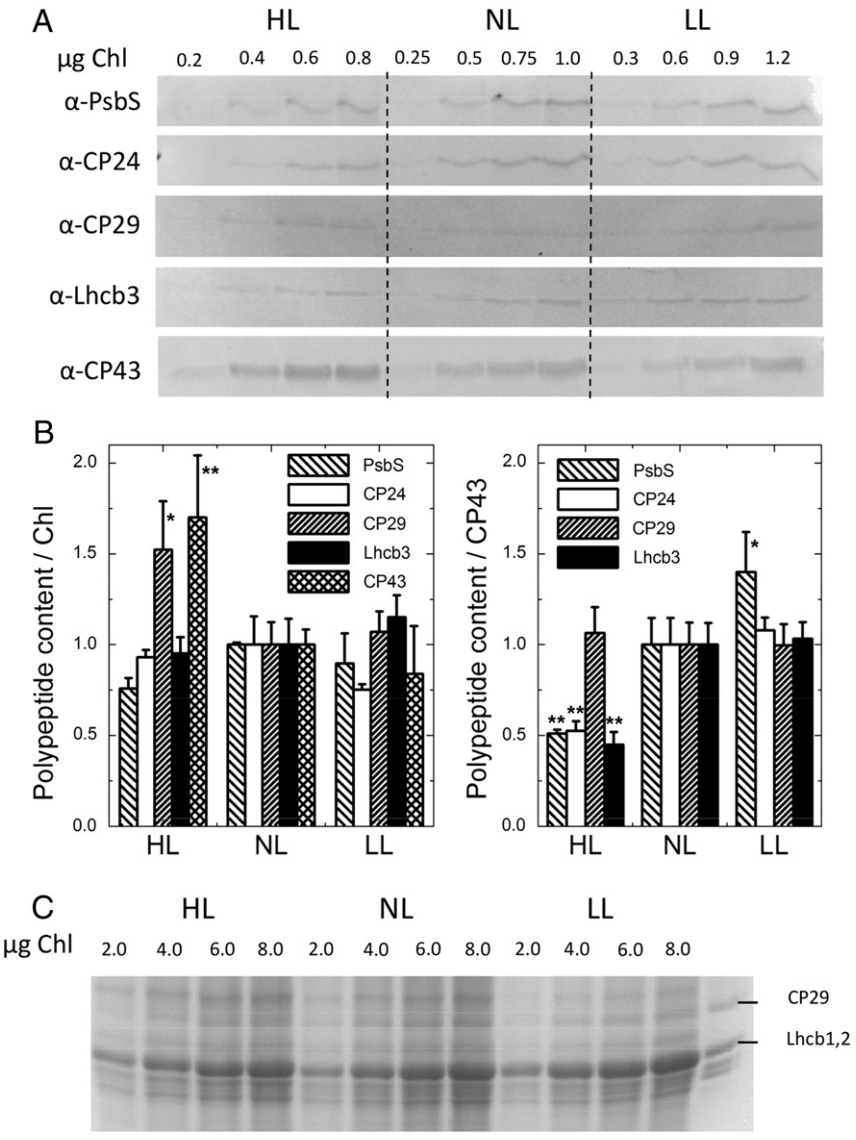

Fig. 1. Quantification of light harvesting proteins of photosystem II and PsbS in plants acclimated to different light conditions. (A) Immunoblotting was performed with antibodies against CP43, CP24, CP29, Lhcb3, and PsbS. The sample was loaded at four different Chls concentrations. Note: it was needed to load different quantities of high light (HL), control (NL) and low light (LL) samples to have similar amounts of CP43 protein. (B) Quantification of immunoblot data. Results are presented relative to the amount of Chl and relative to the PSII core (CP43, quantified by the same method on the same gel; for CP43 per Chl the average from the different gels is shown). Data were normalized to the polypeptide content in the NL sample, the standard deviation is given (n = 3 or 4). Error bars indicate SE (n = 3 or 4); *, ** indicate statistically significant differences at P = 0.05 and P < 0.01 levels, respectively, determined using the Student's test. (C) Determination of Lhcb1 and Lhcb2 content per CP29. SDS-PAGE gel after Coomassie staining. The sample was loaded at four different Chls concentrations to ensure a linearity of the signal.

(see below, Table 1) and probably due to a higher PSII/PSI ratio [30–32]. For that reason, analysis of the polypeptide levels per CP43 was also performed. Obtained data for HL plants indicate an about 50% suppression of both CP24/CP43 and Lhcb3/CP43 content compared to the NL sample, while the amount of CP29/CP43 was unaffected. Analysis of LL plants shows the same amounts of those proteins per PSII core as in NL plants.

Lhcb1 and Lhcb2 levels were quantified by SDS-PAGE and used to estimate the total antenna size per PSII core complex (Fig. 1C, Table 1). In NL plants there are on average 4.8 LHCII trimers per PSII core dimer. As expected, acclimation to HL led to a reduction of the antenna size (3.8 LHCII per PSII core dimer), whereas the opposite effect was observed upon acclimation to LL (7.4 LHCII per PSII core dimer) (Table 1). In line with these results, analysis of the Chl *a*/*b* ratio also indicates a reduction of the Chl b-rich Lhcb antenna in HL plants (chl *a*/*b* = 3.4) compared to NL plants (chl *a*/*b* = 3.0), whereas under LL conditions, plants possess a larger PSII antenna (chl *a*/*b* = 2.7) (Table 1). Considering that there are 4 LHCII per PSII core dimer in the $C_2S_2M_2$ supercomplex, then in NL and

Table 1
Chlorophyll a/b ratio and amounts of trimeric LHCII complexes in plants acclimated to different light intensities. Chl a/b ratio determined by a fitting of the 80% acetone extract spectra (SD < 0.1). Amounts of both bound and "extra" LHCII trimers per PSII core complex were estimated from gels (see Fig. 1 and Section 2.3. for details).

Sample	Chl *a*/*b*	Bound LHCII/PSII core	"Extra" LHCII/PSII core	Total LHCII/PSII core
Low light (LL)	2.7	4	3.4	7.4
Normal light (NL)	3.0	4	0.8	4.8
High light (HL)	3.4	3	0.8	3.8

LL plants there are 0.8 (NL) and 3.4 (LL) "extra" LHCII´s. In HL plants we observed a 50% reduction of CP24 and Lhcb3 (Fig. 1A, B). As Lhcb3 is predominantly or exclusively present in M trimer and that there is one copy per trimer [6,36,37], it can be assumed that in HL there is a 50% reduction in the number of M trimers. This implies that there are 3 LHCII and 0.8 "extra" LHCII per PSII core dimer in HL plants.

The level of PsbS present in membranes of acclimated plants was analyzed. The result was unexpected, as we found a strong reduction of PsbS per PSII core in HL plants (about 50%), whereas its level increased in LL plants in comparison to NL plants (Fig. 1A, B). When the level of PsbS was normalized to the Chl content, as it is usually done, a reduced level of the PsbS was still observed in HL plants (Fig. 1B).

In summary, biochemical data indicate that plant acclimation to HL conditions leads to a reduction of the antenna size of PSII and of the amount of large ($C_2S_2M_2$) PSII supercomplexes. The amount of the "extra" LHCII remains at the same level as in NL plants. Acclimation to LL does not affect the ability of PSII to form large supercomplexes and further, it leads to an increase of the "extra" LHCII pool. Finally, acclimation of plants to HL led to the unexpected significant reduction of PsbS per PSII core, whereas acclimation to LL led to a partial increase of the PsbS level. Interestingly, PsbS was reduced to the same level as CP24 and Lhcb3 proteins.

3.2. Electron microscopy revealed both random and well-ordered organization of PSII complexes in grana membranes

We analyzed the organization of PSII complexes and their antenna proteins in the thylakoid membranes in plants acclimated to HL, NL, and LL. Isolation of thylakoid membranes under stacking conditions was performed after mild solubilization using digitonin. In these conditions, non-appressed membranes are well accessible to detergent and are preferentially solubilized, in contrast to appressed (grana) membranes, which remain intact and appear in the pellet after a short centrifugation. EM of the negatively stained pellet fraction revealed pairs of grana membranes, where characteristic densities of PSII core complexes were clearly visible. Inspection of several hundred of electron micrographs of grana membranes, isolated from plants acclimated to different light intensities, revealed that PSII complexes are mostly randomly distributed, but a subset of them is organized into ordered semi-crystalline arrays (Fig. 2).

3.3. The frequency of semi-crystalline arrays of PSII complexes depends on light conditions

As a semi-crystalline array we consider an array of at least three rows of PSII with at least three PSII complexes in each row. The frequency of semi-crystalline arrays was determined from the number of recorded micrographs where semi-crystalline arrays appeared. The analysis revealed a significant difference between the samples. Under NL and LL conditions, semi-crystalline arrays were found in about 7–8% of the recorded micrographs. In the HL sample, the frequency was significantly reduced to less than 3% (Table 2). Image analysis of sub-areas of 2D arrays revealed that in all analyzed samples the semi-crystalline arrays were composed of PSII $C_2S_2M_2$ supercomplex (Fig. 3). Only under HL conditions, a smaller type of PSII supercomplex (the C_2S_2 complex), was also found to be involved in semi-crystalline arrays formation (Table 1, see below for further details).

3.4. Analysis of semi-crystalline arrays of PSII complexes reveals subtle variations in the crystalline lattice under different light conditions

Semi-crystalline arrays of PSII $C_2S_2M_2$ supercomplexes were further analyzed to see whether different light conditions specifically affect their architecture. At first, semi-crystalline arrays were characterized by the lattice parameters, which were determined from raw micrographs. To be accurate, the lattice constants *a* and *b* of the unit cell, which contains one $C_2S_2M_2$ supercomplex, were calculated over several rows of PSII complexes from center to center of the mass of the PSII core (see Fig. 3A for a definition of the lattice). We also measured the lattice angle α to calculate the unit cell area (Table 3). The lattice constants *a* and *b* fluctuated in a range of 18–22 nm and 24–29 nm, respectively, seemingly without any noticeable dependence on different light conditions. Obtained values are within the range of previously reported data [13].

Secondly, image analysis of small sub-areas of the semi-crystalline arrays was performed to reveal how the PSII supercomplexes interact in these arrays. Fig. 3 shows a gallery of semi-crystalline arrays found under different light conditions. Small insets in the raw electron micrographs represent averaged projection maps of a particular 2D array, which was further assigned by fitting of the pseudo-atomic model of the PSII supercomplex [6]. The assignments indicate overall similar positions and interactions between PSII supercomplexes, independent on light acclimation conditions. A closer look revealed only subtle variations in PSII interactions. For instance, in Fig. 3C and E the cores are lined up in vertical position, whereas in Fig. 3A they slightly incline to the left and in Fig. 3D the inclination is even stronger. This results e.g. in a different interaction between CP24 and CP26 of neighboring PSII supercomplexes (Fig. 3, see white arrowheads).

Another way to compare unit cells is to look at their surface (Table 3). Since the unit cell of the 2D arrays is composed of just one $C_2S_2M_2$ supercomplex, variation in the surface of the unit cell may tell something about the tightness of packing, since the shape of the supercomplex itself is considered to be rigid. There are indeed clear

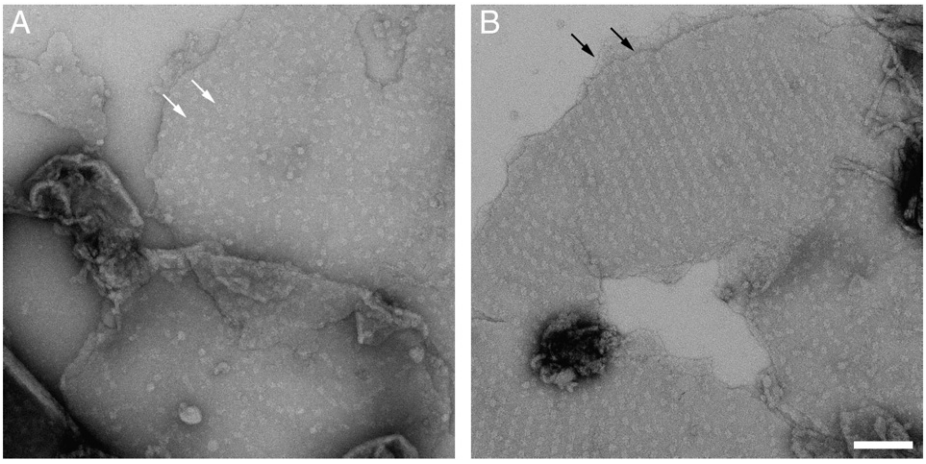

Fig. 2. Examples of electron micrographs of negatively stained pairs of grana membranes isolated from *Arabidopsis thaliana* showing either a random (A) or ordered (B) organization of PSII complexes. The white arrows indicate the characteristic densities of PSII core complexes; the black arrows indicate a single piece of a membrane layer. Scale bar is 100 nm.

Table 2
Frequency and type of semi-crystalline arrays of PSII supercomplexes found in grana membranes of the HL, LL, and NL plants. A total number of recorded micrographs is indicated. Under HL conditions, a majority of semi-crystalline arrays were formed by the C2S2M2 supercomplex (about 90%); only 10% of semi-crystalline arrays were formed by the C2S2 complex.

Sample	HL	LL	NL
Number of recorded micrographs	545	378	555
Micrographs with 2D PSII arrays [%]	2.8	8.5	7.4
Type of PSII supercomplexes involved in a 2D array formation	$C_2S_2M_2$ C_2S_2	$C_2S_2M_2$	$C_2S_2M_2$

differences in the packing surfaces. The strongest, statistically significant difference in the averaged surface is between the LL and NL crystals, with averaged surface of 503 nm^2 and 524 nm^2, respectively (Table 3). The average HL crystal has a surface of 519 nm^2, but only a small number has been determined, due to the low frequency. The smaller surface of the LL crystals indicates a closer packing of the PSII supercomplexes under LL conditions.

3.5. Randomly organized PSII supercomplexes undergo specific rearrangements in the membrane upon acclimation to different light conditions

The major part of the electron micrographs (>90%) shows randomly distributed PSII complexes (see Fig. 2A). To see whether different light conditions have an influence on the random distribution, both the minimal distance between neighboring PSII complexes and their density in the membrane area were determined.

Minimal distances between randomly distributed PSII complexes under HL, LL, and NL conditions were calculated for about 5000 particles which were manually selected from electron micrographs (see Section 2.4. for details). Analysis of HL and NL samples indicates a very similar minimal distance distribution. Most PSII complexes have a minimal distance to the closest neighbor of about 22 nm (Fig. 4). Analysis of LL sample revealed a slightly different distribution with frequency maximums between 19 nm and 21 nm and amplitudes about 20% lower compared to HL and NL samples. Further, LL conditions led to a larger separation of PSII complexes in the membrane, which can be seen from a larger population of PSII complexes with a minimal distance over 26 nm (Fig. 4). Interestingly, LL conditions do not preclude close contact between PSII complexes, as the frequency of PSII complexes with minimal distances below e.g. 18 nm was very similar to the distribution obtained for the HL and NL samples.

Analysis of HL and NL samples shows a rather uniform distribution of PSII complexes in the grana membranes with a density of about 1400 to 1900 PSII complexes per μm^2 (Fig. 5). Analysis of LL plants revealed a considerably lower density, which typically reached a value between 600 and 1300 PSII complexes per μm^2 (Fig. 5). Moreover, electron micrographs of the LL sample revealed a tendency of PSII complexes to specifically associate into rows (Fig. 5C), as observed previously [20].

4. Discussion

4.1. Both bound and "extra" LHCII undergo a specific regulation under plant acclimation to different light intensities

Analysis of plants acclimated to different light intensities indicates a very specific regulation of PSII antenna size at the level of individual proteins. In line with previously published data [31,32], our work confirms a down-regulation of Lhcb1–3 and CP24 proteins in HL plants, while Lhcb1,2 were up-regulated in LL plants.

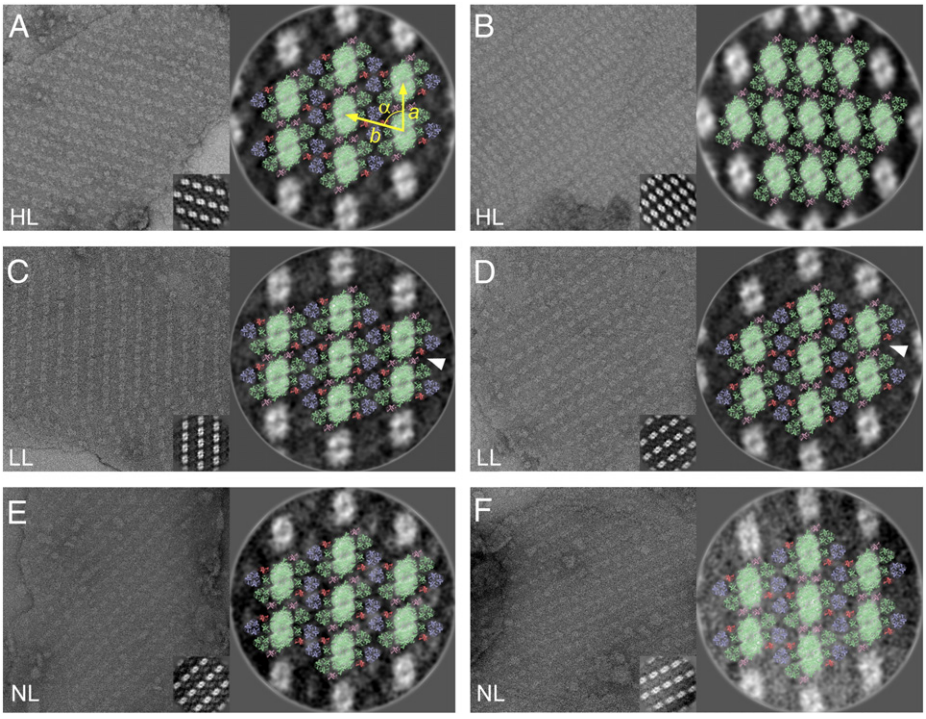

Fig. 3. A gallery of electron micrographs of negatively stained grana membranes with semi-crystalline arrays of PSII supercomplexes from *Arabidopsis thaliana* grown under high light (HL) (A, B), low light (LL) (C, D) and under optimal light intensity (NL) (E, F). The insets show the results of image analysis of sub-areas of ordered arrays of PSII supercomplexes selected from the electron micrographs. Averaged projections were assigned by the fitting of the structural pseudo-atomic model of the PSII $C_2S_2M_2$ supercomplex according to [6] (PSII core complex, the minor antenna CP29 and S-type of light harvesting trimer are depicted in light green, M-type of light harvesting trimer, minor antennae CP24 and CP26 are depicted in light blue, dark salmon and light pink, respectively). Semi-crystalline arrays consist of $C_2S_2M_2$ type of PSII supercomplex. In the high light sample, semi-crystalline array of the C_2S_2 type of PSII supercomplex was also found (B). White arrowheads in (C) and (D) indicate a different interaction between minor antenna proteins CP26 and CP24. The right part of Fig. (A) indicates the definition of lattice parameters, a, b, and the intermediate angle α.

Table 3
Lattice parameters of semi-crystalline arrays. In total, 93 semi-crystalline arrays of the PSII C2S2M2 supercomplexes from HL, LL, and NL plants were characterized. Presented are the unit cell parameters of the lattice and the surface of the unit cell. Lattices are sorted by (1) an ascending angle α between lattice parameters a and b and (2) the ascending length of a (see Fig. 3 for lattice parameters assignment). No. value indicates a number of semi-crystalline arrays with given lattice parameters. Average values of the surface of the lattice cells are 519 nm^2, 503 nm^2 ***, and 524 nm^2 for HL, LL and NL plants, respectively. Asterisks indicate a statistically significant difference between LL and NL plants at $P<0.001$ determined using the Student's test.

	HL				LL				NL			
α	*a*	*b*	Surface	No.	*a*	*b*	Surface	No.	*a*	*b*	Surface	No.
[°]	[nm]	[nm]	[nm^2]		[nm]	[nm]	[nm^2]		[nm]	[nm]	[nm^2]	
65					19	28	490	1				
					20	28	509	1				
66									20	29	528	1
67	21	28	529	1	18	29	490	1	20	28	517	2
					19	28	488	2	21	27	523	1
68	21	28	544	2	19	28	495	5	19	28	513	1
					20	28	502	2	20	28	507	1
69					19	28	499	1	20	29	532	6
					20	28	510	1	21	28	541	2
									22	26	552	1
70					19	28	508	1	19	28	502	1
					20	28	508	4	20	28	517	3
71	20	27	515	2	19	28	503	2	19	28	507	1
	22	26	533	1	21	26	527	1	20	27	517	3
									21	28	551	1
72	20	26	500	1	20	28	518	2	20	26	499	1
	21	27	530	3	21	25	498	3	21	27	533	1
									22	25	530	1
73	21	26	521	1	20	25	490	1	19	28	512	2
					21	26	503	1	20	26	511	1
									21	26	527	3
									22	26	535	1
74	21	25	507	1	20	26	511	3	21	26	524	2
					21	26	525	1				
75	20	25	491	1	20	25	497	1	20	26	514	1
	21	25	498	1	21	25	510	1	21	26	529	2
76									21	26	535	1
77	21	24	489	1	20	25	490	1				
78					18	27	488	1				
81					20	26	520	1				

In HL acclimated plants, immunoblot titration shows about 50% reduction of both Lhcb3 and CP24 proteins (Fig. 1A, B), indicating a 50% reduction of the M trimer. This can fully account for the observed reduction of Lhcb1 and Lhcb2 proteins (which form 2/3 of the M trimer). Down-regulation of the M trimer should lead to the reduction of PSII–LHCII supercomplex (the $C_2S_2M_2$ type) into smaller forms (e.g.C_2S_2M or C_2S_2). Indeed, semi-crystalline arrays of the C_2S_2 type of PSII supercomplex were observed only in HL plants (Fig. 3B). Interestingly, the "extra" LHCII pool remains at the same level as in NL plants. On the contrary, in LL plants, the stoichiometry between the components of the PSII-LHCII supercomplex remains unaffected (Fig. 1A,B). This implies that the strong up-regulation of Lhcb1 and 2 leads to an enlargement of the "extra" LHCII pool. Indeed, EM analysis of LL acclimated plants shows large areas without PSII complexes (Fig. 5C), which most likely represent LHCII regions. In summary, our data indicate that PSII-associated antenna proteins are the main targets of regulation in HL

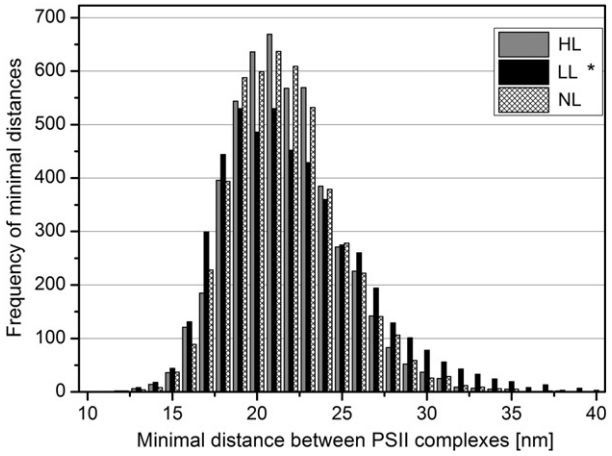

Fig. 4. A frequency of minimal distances between PSII complexes determined from electron micrographs of grana membranes isolated from the high-light (HL), low-light (LL), and control (NL) samples. About 5000 single particles were analyzed for each type of the sample. * indicates statistically significant difference at $P = 0.05$ determined using the Student's test.

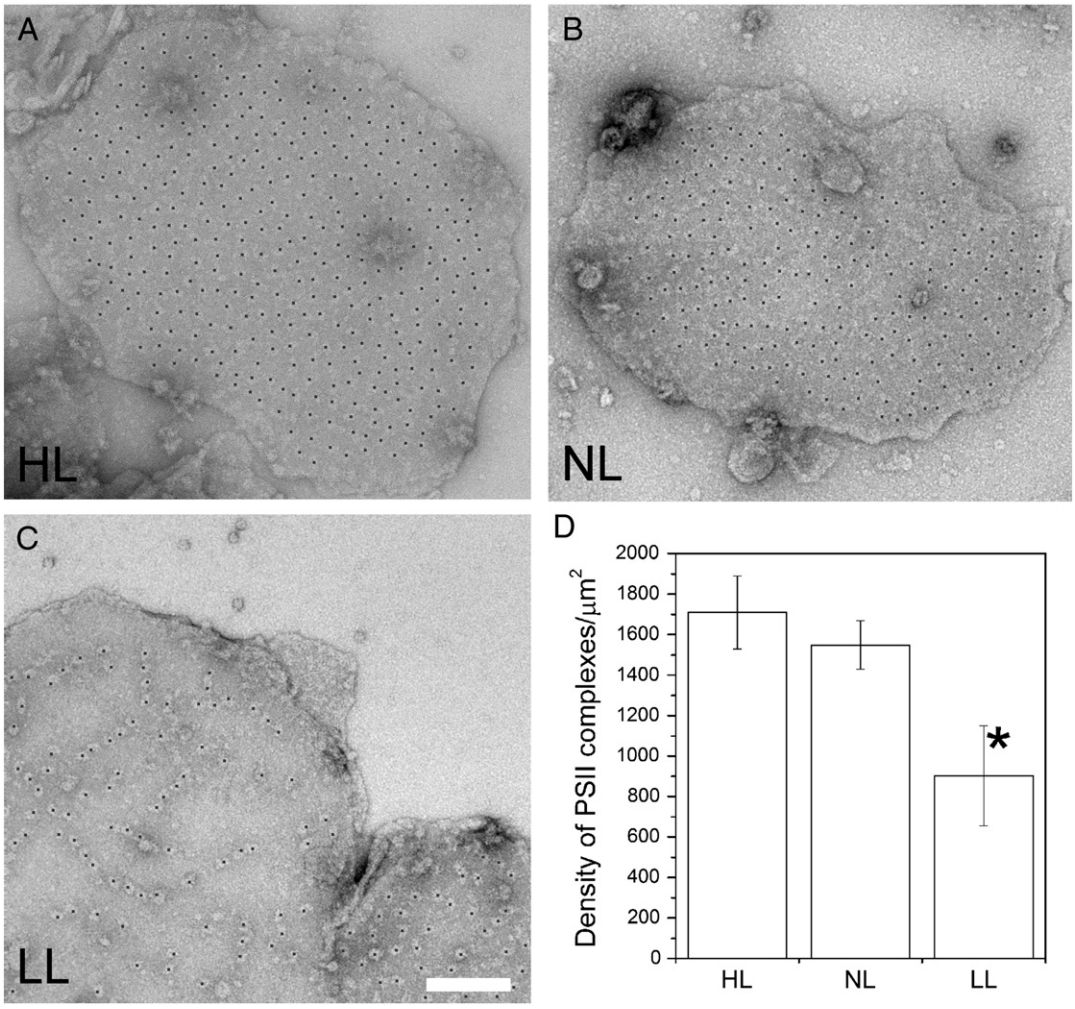

Fig. 5. Density of PSII complexes (grey dots) in the grana membranes of the high-light (HL) (A), low-light (LL) (B), and control (NL) (C) samples. Scale bar is 100 nm. (D) Density of PSII complexes determined for 8 electron micrographs of grana membranes from the HL, LL, and NL samples. A significantly different value from control sample is marked with an asterisk. Error bars indicate SE (n = 8); * indicates statistically significant difference at P = 0.05 determined using the Student's test.

plants. Plant acclimation to LL is accompanied by a regulation of the "extra" LHCII pool, whereas the antenna bound to PSII remains unaffected.

4.2. Frequency of semi-crystalline arrays of PSII is strongly reduced in HL plants

In many structural studies different EM techniques have highlighted the enigmatic organization of PSII complexes into semi-crystalline arrays in the thylakoid membrane. Our data show that the frequency of PSII 2D arrays in the thylakoid membrane depends on growing light intensity. We observed a significant reduction in frequency of PSII 2D arrays in HL plants (about three times) compared to NL (Table 2). Acclimation of plants to LL led to only a minor increase in the frequency of semi-crystalline arrays compared to NL plants. Thus our data did not prove a strong stimulating effect of low light intensity on a formation of ordered arrays of PSII in the membrane as was reported earlier [20]. A possible explanation of this discrepancy is in the way of defining 2D arrays. In contrast to work of Kirchhoff et al. [20], we did not consider single rows of PSII complexes as 2D arrays, although such rows were frequently seen in LL plants (Fig. 5C).

What can be the trigger for a reduced frequency of 2D arrays observed in HL plants? One possibility is the effect of PsbS. It was reported that an elevated level of PsbS in *Arabidopsis* mutant L17 completely suppresses the formation of semi-crystalline arrays, whereas a lack of the PsbS protein in *Arabidopsis npq4* mutant increases their frequency [22,23]. However, the above observation is seemingly inconsistent with our data, as acclimation of plants to HL led to a decrease in both PsbS level (Fig. 1) and frequency of semi-crystalline arrays (Table 2). Thus, although PsbS has an influence on the 2D array frequency, the array decrease observed here is not due to an increase in the content of PsbS. Before we discuss this topic further on, we like to point out that our finding of a reduced level of PsbS in HL plants is in disagreement with other reports, where either nearly unchanged [40,41] or strongly increased levels of PsbS were reported [32,42]. Although, part of observed discrepancies in the determination of PsbS level in HL plants is due to the normalization method (either to PSII core protein or Chl content), it should be mentioned that in our case the amount of PsbS decreases in HL plants in respect to both the core protein and the total chl content.

In general, one can assume that the formation of 2D arrays in the thylakoid membrane requires a locally homogenous population of PSII supercomplexes. Indeed, in the case of barley PSI-less mutant *viridis zb63*, where PSII complexes are only present in the form of C_2S_2, the grana membranes are organized into large semi-crystalline arrays of up to 0.7 μm in diameter [43,44]. Similarly a very high frequency of semi-crystalline was observed in the CP24KO mutant, where only C_2S_2 complexes were present [45,46]. The presence of a mixture of different types of PSII supercomplexes, like e.g. $C_2S_2M_2$, C_2S_2M, and C_2S_2, can hamper the formation of semi-crystalline arrays. In HL plants, we observed a reduction of CP24 and components of the M trimer, which

implies the presence of smaller PSII supercomplexes than the $C_2S_2M_2$ supercomplex in the thylakoid membrane. Further, analysis of the LL sample indicates that the presence of the "extra" LHCII proteins is not hampering the formation of semi-crystalline arrays. Therefore, we can conclude that the structural heterogeneity of the PSII supercomplexes is the main reason for a lower frequency of PSII semi-crystalline arrays in the thylakoid membrane.

4.3. Unit cell surface of semi-crystalline array of PSII is significantly reduced in LL plants

In all previous EM studies where image processing was performed on 2D arrays, final average 2D maps of semi-crystalline arrays were obtained by taking together the information of many membrane patches. In this study, however, we analyzed for the first time the lattices of *single* crystals.

A thorough analysis of 2D arrays and their assignment by a fitting of the pseudo-atomic model of the PSII supercomplex revealed a significant difference in a tightness of packing of PSII supercomplexes. A smaller unit cell surface indicates a closer contact between PSII supercomplexes in LL plants compared to NL/HL plants (Table 3). Apparently, LL plants prefer (and benefit) keeping PSII complexes tightly clustered either in semi-crystalline arrays or row-like structures. This can be relevant for an optimal performance of the photosynthetic apparatus under light limiting conditions, facilitating energy transfer between supercomplexes. On the contrary, a wider spacing between PSII supercomplexes (a larger unit cell surface) in NL and HL plants can facilitate the diffusion of PQ molecules under light saturating conditions. It remains unclear what helps plants to control the spacing between supercomplexes. Analysis of the lattice parameters revealed their independence on light acclimation conditions (Table 3). Therefore the spacing is not controlled by a specific interaction between PSII supercomplexes. We can speculate that the lipid to protein ration is probably of relevance.

Acknowledgements

This work was supported by The Netherlands Organisation for Scientific Research (NWO), Earth and Life Sciences (ALW), through a Vici grant (to R.C.); grant no. ED0007/01/01 Centre of the Region Haná for Biotechnological and Agricultural Research and no. OP VK CZ.1.07/2.3.00/20.0057 (to R.K.).

References

[1] P.Å. Albertsson, A quantitative model of the domain structure of the photosynthetic membrane, Trends Plant Sci. 6 (2001) 349–354.
[2] N. Nelson, C.F. Yocum, Structure and function of Photosystems I and II, Annu. Rev. Plant Biol. 57 (2006) 521–565.
[3] R. Kouřil, J.P. Dekker, E.J. Boekema, Supramolecular organization of photosystem II in green plants, Biochim. Biophys. Acta 1817 (2012) 2–12.
[4] E.J. Boekema, B. Hankamer, D. Bald, J. Kruip, J. Nield, A.F. Boonstra, J. Barber, M. Rögner, Supramolecular structure of the photosystem II complex from green plants and cyanobacteria, Proc. Natl. Acad. Sci. U. S. A. 92 (1995) 175–179.
[5] E.J. Boekema, H. van Roon, J.P. Dekker, Specific association of photosystem II and light-harvesting complex II in partially solubilized photosystem II membranes, FEBS Lett. 424 (1998) 95–99.
[6] S. Caffarri, R. Kouřil, S. Kereïche, E.J. Boekema, R. Croce, Functional architecture of higher plant photosystem II supercomplexes, EMBO J. 28 (2009) 3052–3063.
[7] R. Croce, H. van Amerongen, Light-harvesting and structural organization of photosystem II: from individual complexes to thylakoid membrane, J. Photochem. Photobiol. B 104 (2011) 142–153.
[8] G.F. Peter, J.P. Thornber, Biochemical composition and organization of higher plant photosystem II light-harvesting pigment-proteins, J. Biol. Chem. 266 (1991) 16745–16754.
[9] K. Broess, G. Trinkunas, A. van Hoek, R. Croce, H. van Amerongen, Determination of the excitation migration time in photosystem II — consequences for the membrane organization and charge separation parameters, Biochim. Biophys. Acta 1777 (2008) 404–409.
[10] B. van Oort, M. Alberts, S. de Bianchi, L. Dall´Osto, R. Bassi, G. Trinkunas, R. Croce, H. van Amerongen, Effect of antenna-depletion in photosystem II on excitation energy transfer in *Arabidopsis thaliana*, Biophys. J. 98 (2010) 922–931.
[11] K.R. Miller, G.J. Miller, K.R. McIntyre, Light-harvesting chlorophyll-protein complex of photosystem 2. Its location in photosynthetic membrane, J. Cell Biol. 71 (1976) 624–638.
[12] L.A. Staehelin, Chloroplast structure: from chlorophyll granules to supra-molecular architecture of thylakoid membranes, Photosynth. Res. 76 (2003) 185–196.
[13] J.P. Dekker, E.J. Boekema, Supramolecular organization of thylakoid membrane proteins in green plants, Biochim. Biophys. Acta 1706 (2005) 12–39.
[14] H. Kirchhoff, I. Tremmel, W. Haase, U. Kubitscheck, Supramolecular photosystem II organization in grana thylakoid membranes: evidence for a structured arrangement, Biochemistry 43 (2004) 9204–9213.
[15] H. Kirchhoff, S. Lenhert, C. Büchel, L. Chi, J. Nield, Probing the organization of photosystem II in photosynthetic membranes by atomic force microscopy, Biochemistry 47 (2008) 431–440.
[16] K. Sznee, J.P. Dekker, R.T. Dame, H. van Roon, G.J. Wuite, R.N. Frese, Jumping mode atomic force microscopy on grana membranes from spinach, J. Biol. Chem. 256 (2011) 39164–39171.
[17] E.J. Boekema, J.F.L. van Breemen, H. van Roon, J.P. Dekker, Arrangement of photosystem II supercomplexes in crystalline macrodomains within the thylakoid membrane of green plant chloroplasts, J. Mol. Biol. 301 (2000) 1123–1133.
[18] A.E. Yakushevska, P.E. Jensen, W. Keegstra, H. van Roon, H.V. Scheller, E.J. Boekema, J.P. Dekker, Supermolecular organization of photosystem II and its associated light-harvesting antenna in *Arabidopsis thaliana*, Eur. J. Biochem. 268 (2001) 6020–6021.
[19] M.P. Garber, P.L. Steponkus, Alterations in chloroplast thylakoids during cold acclimation, Plant Physiol. 57 (1976) 681–686.
[20] H. Kirchhoff, W. Haase, S. Wegner, R. Danielsson, R. Ackermann, P.A. Albertsson, Low-light-induced formation of semicrystalline photosystem II arrays in higher plant chloroplasts, Biochemistry 46 (2007) 11169–11176.
[21] A.V. Ruban, M. Wentworth, A.E. Yakushevska, J. Andersson, P.J. Lee, W. Keegstra, J.P. Dekker, E.J. Boekema, S. Jansson, P. Horton, Plants lacking the main light-harvesting complex retain photosystem II macro-organization, Nature 421 (2003) 648–652.
[22] S. Kereïche, A.Z. Kiss, R. Kouřil, E.J. Boekema, P. Horton, The PsbS protein controls the macro-organisation of photosystem II complexes in the grana membranes of higher plant chloroplasts, FEBS Lett. 584 (2010) 759–764.
[23] T.K. Goral, M.P. Johnson, C.D. Duffy, A.P. Brain, A.V. Ruban, C.W. Mullineaux, Light-harvesting antenna composition controls the macrostructure and dynamics of thylakoid membranes in *Arabidopsis*, Plant J. 69 (2012) 289–301.
[24] B. Daum, D. Nicastro, J. Austin, J.R. McIntosh, W. Kühlbrandt, Arrangement of photosystem II and ATP synthase in chloroplast membranes of spinach and pea, Plant Cell 22 (2010) 1299–1312.
[25] R. Kouřil, G.T. Oostergetel, E.J. Boekema, Fine structure of granal thylakoid membrane organization using cryo electron tomography, Biochim. Biophys. Acta 1807 (2011) 368–374.
[26] A.V. Ruban, M.P. Johnson, C.D. Duffy, The photoprotective molecular switch in the photosystem II antenna, Biochim. Biophys. Acta 1817 (2012) 167–181.
[27] J. Minagawa, State transitions — the molecular remodeling of photosynthetic supercomplexes that controls energy flow in the chloroplast, Biochim. Biophys. Acta 1807 (2011) 897–905.
[28] M.P. Johnson, T.K. Goral, C.D.P. Duffy, A.P.R. Brain, C.W. Mullineaux, A.V. Ruban, Photoprotective energy dissipation involves the reorganization of photosystem II light-harvesting complexes in the grana membranes of spinach chloroplasts, Plant Cell 23 (2011) 1468–1479.
[29] J.M. Anderson, Photoregulation of the composition, function, and structure of thylakoid membranes, Annu. Rev. Plant Physiol. 37 (1986) 93–136.
[30] J.M. Anderson, W.S. Chow, D.J. Goodchild, Thylakoid membrane organization in sun/shade acclimation, Aust. J. Plant Physiol. 15 (1988) 11–26.
[31] S. Bailey, R.G. Walters, S. Jansson, P. Horton, Acclimation of *Arabidopsis thaliana* to the light environment: the existence of separate low light and high light responses, Planta 213 (2001) 794–801.
[32] M. Ballottari, L. Dall´Osto, T. Morosinotto, R. Bassi, Contrasting behavior of higher plant photosystem I and II antenna systems during acclimation, J. Biol. Chem. 282 (2007) 8947–8958.
[33] H.H. Robinson, C.F. Yocum, Cyclic photophosphorylation reactions catalyzed by ferredoxin, methyl viologen and anthraquinone sulfonate — use of photochemical-reactions to optimize redox poising, Biochim. Biophys. Acta 590 (1980) 97–106.
[34] H. Schagger, Tricine-SDS-PAGE, Nat. Protoc. 1 (2006) 16–22.
[35] S.W. Hogewoning, E. Wientjes, P. Douwstra, G. Trouwborst, W. van Ieperen, R. Croce, J. Harbinson, Photosynthetic quantum yield dynamics: from photosystems to leaves, Plant Cell 24 (2012) 1921–1935.
[36] P. Dainese, R. Bassi, Subunit stoichiometry of the chloroplast photosystem II antenna system and aggregation state of the component chlorophyll a/b binding proteins, J. Biol. Chem. 266 (1991) 8136–8142.
[37] B. Hankamer, J. Nield, D. Zheleva, E.J. Boekema, S. Jansson, J. Barber, Isolation and biochemical characterisation of monomeric and dimeric photosystem II complexes from spinach and their relevance to the organisation of photosystem II in vivo, Eur. J. Biochem. 243 (1997) 422–429.
[38] E. Wientjes, G.T. Oostergetel, S. Jansson, E.J. Boekema, R. Croce, The role of Lhca complexes in the supramolecular organization of higher plant photosystem I, J. Biol. Chem. 284 (2009) 7803–7810.
[39] G.T. Oostergetel, W. Keegstra, A. Brisson, Automation of specimen selection and data acquisition for protein electron crystallography, Ultramicroscopy 74 (1998) 47–59.
[40] M. Lindahl, C. Funk, J. Webster, S. Bingsmark, I. Adamska, B. Andersson, Expression of ELIPs and PS II-S protein in spinach during acclimative reduction of the photosystem II antenna in response to increased light intensities, Photosynth. Res. 54 (1997) 227–236.

[41] Y. Mishra, H.J. Jänkänpää, A.Z. Kiss, C. Funk, W.P. Schröder, S. Jansson, Arabidopsis plants grown in the field and climate chambers significantly differ in leaf morphology and photosystem components, BMC Plant Biol. 12 (2012) 6.
[42] M. Tikkanen, M. Piippo, M. Suorsa, S. Sirpiö, P. Mulo, J. Vainonen, A.V. Vener, Y. Allahverdiyeva, E.M. Aro, State transitions revised — a buffering system for dynamic low light acclimation of *Arabidopsis*, Plant Mol. Biol. 62 (2006) 779–793.
[43] D.J. Simpson, Freeze-fracture studies on barley plastid membranes. VI. Location of the P700-chlorophyll a-protein 1, Eur. J. Cell Biol. 31 (1983) 305–314.
[44] T. Morosinotto, R. Bassi, S. Frigerio, G. Finazzi, E. Morris, J. Barber, Biochemical and structural analysis of a higher plant photosystem II supercomplex of a photosystem I-less mutant of barley, FEBS J. 273 (2006) 4616–4630.
[45] L. Kovács, J. Damkjær, S. Kereïche, C. Ilioaia, A.V. Ruban, E.J. Boekema, S. Jansson, P. Horton, Lack of the light-harvesting complex CP24 affects the structure and function of the grana membranes of higher plant chloroplasts, Plant Cell 18 (2006) 3106–3120.
[46] S. de Bianchi, L. Dall´Osto, G. Tognon, T. Morosinotto, R. Bassi, Minor antenna proteins CP24 and CP26 affect the interactions between photosystem II subunits and the electron transport rate in grana membranes of *Arabidopsis*, Plant Cell 20 (2008) 1012–1028.